Hindawi
Journal of Advanced Transportation
Volume 2022, Article ID 2006978, 8 pages
https://doi.org/10.1155/2022/2006978

Research Article

Optimization of the Reversible Lane considering the Relationship between Traffic Capacity and Number of Lanes

Jianrong Cai,[1] Jianhui Wu,[2] Zhixue Li,[1] Qiong Long,[1] Zhaoming Zhou,[1] Jie Yu,[1] and Xiangjun Jiang[3]

[1]*School of Civil Engineering, Hunan City University, Yiyang, Hunan 413000, China*
[2]*School of Information Science and Technology, Hunan Institute of Science and Technology, Yueyang 414006, China*
[3]*Department of Traffic Management, Hunan Police Academy, Changsha, Hunan 410000, China*

Correspondence should be addressed to Jianhui Wu; wjh_hnist@163.com

Received 11 March 2022; Revised 10 April 2022; Accepted 15 April 2022; Published 28 April 2022

Academic Editor: Elżbieta Macioszek

To make full use of road resources, improve the operation efficiency of the road network system, and alleviate the coexistence between traffic congestion and road resources idle caused by the traffic tidal phenomenon, the impact of the number of lanes on traffic capacity is examined, and the mixed-integer bilevel programming model for reversible lane optimization is established with the aim to minimalize the total travel time of the system. Taking a test road network as an example, the influence of the reversible lane optimization on characteristic values of sections, the route travel time between OD pairs, and the total time of the system are analyzed. The results indicate that the reversible lane optimization can make full use of the idle road resources and make the road network structure match the travel demands better, and the system index after the reversible lane optimization is obviously better than the original system index.

1. Introduction

Urban traffic flow has two typical characteristics. One is temporal asymmetry on some roads and another is spacial asymmetry on some roads. As more and more urban residents choose to work in the city center and live in the suburbs, urban traffic has obvious tidal characteristics. During the peak hours, the flow in one direction of the lanes is greater than the capacity resulting in congestion, while the lanes in the other direction are not fully utilized resulting in the idleness of road resources, and the traffic system is in a state of congestion and inefficient operation.

There have been a large number of theoretical and simulation studies of traffic systems in order to solve the problem of congestion and achieve high traffic efficiency (e.g., Li et al. [1]). And the implementation of reversible lanes which adjusts the road resources in the light traffic flow direction to the heavy traffic flow direction is an effective measure to solve the problem of tidal traffic congestion and improve the operation efficiency of the whole road network system greatly, without changing the road structure, control facilities, or traffic infrastructure (e.g., Wong et al. [2], Jiang et al. [3], Yu et al. [4], Wolshon et al. [5], and Golub et al. [6]).

Zhang et al. [7] established the network reserve capacity model and demonstrated that reversible lane can greatly improve the reserve capacity of the road network. In the study of Li et al. [8], in order to make the periodic flow direction of the reversible traffic system change more smoothly, a reversible lane adjustment method suitable for urban trunk roads from off-peak time to peak time is proposed. Hausknecht et al. [9] pointed out that the reversible lane system can increase the capacity of congested sections, effectively reduce traffic congestion in peak hours, and facilitate the emergency evacuation of travel users. Wolshon et al. [10] analyzed the problems that can be solved by the setting of reversible lanes and believed that the cost, advantages, and disadvantages of various design schemes and the long-term benefits of the whole transportation system should be comprehensively considered when

planning reversible lanes. Waleczek et al. [11] studied the effectiveness, feasibility, and safety issues of reversible lanes and considered that the reversible lane system is a practical and safe intelligent traffic management tool.

Yue et al. [12] demonstrated the necessity and feasibility of implementing reversible lane during the Shanghai World Expo and preliminarily discussed the specific implementation scheme. Wang et al. [13] developed an optimization model to decide the number and scheduling rules of the reversible lanes of container gates under the constraints of limited spaces and imbalanced traffic volumes. Sheu et al. [14] analyzed the potential of applying lane reversal techniques to alleviate temporary congestion caused by traffic incidents and formulated a discrete-time nonlinear stochastic model with the estimation of lane-changing fractions for real-time incident management. Xiao et al. [15] focused on disseminating messages under global traffic information and studied the cooperative bargain for the separation of traffic flows in smart reversible lanes so as to make consistent movements when separating the flows. Mao et al. [16] proposed a real-time dynamic reversible lane scheme in the Intelligent Cooperative Vehicle Infrastructure System (CVIS) which was applied to determine the number of lanes and the timing of lane changes.

Bilevel programming model is increasingly used in the field of reversible lane optimization, typically the upper-level decides on the lanes, changing their performance depending on the lower-level travelers' routing decisions (e.g., Magnanti et al. [17]). Shi et al. [18] established a master-slave bilevel programming model with the goal of reducing the total travel cost in the peak period of the urban transportation network and reducing the management cost of reversible lane setting. Gao et al. [19] and Zhang et al. [20] constructed a bilevel programming model of reversible lane optimization with the goal of minimizing the total impedance of the road network, in which the upper level is the reversible lane setting scheme of the traffic management department and the lower level is the user optimal allocation of travel users according to the set scheme. Lu theoretically analyzed the behaviors of the players involved in the leader-follower strategic game and established a bilevel programming model considering the game equilibrium between road users and traffic controllers (e.g., Lu et al. [21]).

Di defines a coupling measure to quantify the relationship between network structure and demand structure, with the aim to maximize the coupling measure, and a nonlinear bilevel mixed-integer programming model is established to find the optimal lane combination strategy in the considered network from the viewpoint of systematology (e.g., Di et al. [22]). When the goal of the upper level is the same as the lower level, the problem can be formulated as a single-level programming model (e.g., Conceio et al. [23] and Cai et al. [24]).

The abovementioned studies on reversible lanes are based on the ideal assumption that the capacity of the road section is absolutely proportional to the number of lanes. But, in fact, with the increase in the number of lanes, the average capacity of each lane decreases accordingly. When the number of lanes is more than 4, the average capacity of each lane even decreases by more than 16%. Ignoring this practical impact may lead to a large deviation between the model and the actual situation (e.g., Yang et al. [25]). Therefore, this paper takes maintaining the normal traffic in the direction of light traffic flow during the implementation of reversible lanes as the basic premise, considers the reduction impact of the number of lanes on the traffic capacity of the road section, and studies the optimal setting scheme of the reversible lanes from the perspective of system optimization in order to ensure the effectiveness of the whole transportation system and alleviate the coexistence of traffic congestion and idle road resources.

This manuscript is structured as follows. After the introduction, Section 2 is the analysis of the relationship between road capacity and the number of lanes. In Section 3, the bilevel programming model for reversible lane optimization is established. In Section 4, the feasibility of this optimization model and its solution algorithm is verified. In Section 5, the calculations and analysis of numerical example are given. In Section 6, the conclusions of this research are drawn.

2. Analysis of the Relationship between Traffic Capacity and Number of Lanes

The capacity of the road section increases with the increase of the number of lanes, but with the increase of the number of lanes, the opportunity for vehicle lane-changing increases accordingly, the mutual interference between vehicles increases, and the increase of the actual traffic capacity of the road section decreases marginally with the increase of the number of lanes.

Understanding the effect of lane-changing on traffic is an important topic in designing optimal traffic control systems (e.g., Li et al. [26]). According to Xiaobao Yang et al.'s [27] research results, if the average capacity per lane of 2 lane section is c_2 and the lane-changing frequency is $a_2\,(a_2 = -0.224)$, the average capacity per lane of n lane section is c_n.

$$c_n = c_2 e^{a_2(n-2)/n}, \quad n \geq 2. \tag{1}$$

In specific planning, the lane number correction coefficient of single-lane section is 1, and the lane number correction coefficient of 2 lane section is 1.87 (e.g., Wang et al. [28]). If the traffic capacity of 1 lane is set as c_1, average capacity per lane of 2 lane section is c_2.

$$c_2 = \frac{1.87 c_1}{2} = 0.935 c_1. \tag{2}$$

The average capacity per lane of n lane section is c_n.

$$c_n = \begin{cases} 0.935 c_1 e^{a_2(n-2)/n}, & n \geq 2 \\ c_1 & n = 1 \end{cases}. \tag{3}$$

Take the unit impulse sequence as

$$\delta(n-1) = \begin{cases} 1, & n = 1 \\ 0, & \text{others} \end{cases}. \tag{4}$$

Table 1: Average capacity per lane.

Number of lanes	1	2	3	4	5	6	7	n
Average capacity per lane	c_a	0.935 c_a	0.8678 c_a	0.8359 c_a	0.8174 c_a	0.8053 c_a	0.7967 c_a	0.935 $e^{a_2(n-2)/n}c_a$

Take the unit step sequence as

$$u(n-2) = \begin{cases} 1, & n \geq 2 \\ 0, & \text{others} \end{cases}. \tag{5}$$

Then, the average capacity per lane of the n lane section can be obtained as

$$c_n = \delta(n-1)c_1 + u(n-2)0.935c_1 e^{a_2(n-2)/n}. \tag{6}$$

3. Bilevel Programming Model for Reversible Lane Optimization

Note that the node set of the whole road network is N, the road section set is A, and the OD (origin destination) pair set is w. Assuming that section $a \in A$ has a corresponding reverse section $\overline{a}$, note that the two-way section $\ddot{a}$ is composed of section a and section $\overline{a}$. x_a represents the flow of section a, l_a represents the number of lanes of section a, C_a represents the capacity of section a, and c_a represents the capacity of a single lane of section a. Note that the free travel time of section a is t_a^0, the travel time of each section is $t_a(x_a, l_a)$, and its functional form adopts BPR formula:

$$t_a(x_a, l_a) = t_a^0\left[1 + \alpha\left(\frac{x_a}{C_a}\right)^{\beta}\right], \quad a \in A, \tag{7}$$

where α and β are undetermined parameters and C_a can be obtained as

$$C_a = l_a \cdot c_n, \quad a \in A. \tag{8}$$

According to formula (6), the average capacity per lane of n lane section can be obtained as shown in Table 1.

It is assumed that all travelers have the decision to select the path with the minimum travel time, and the road network reaches the user equilibrium state. For the reversible lane system, the traffic management department can optimize the allocation of road resources through the adjustment of the number of lanes so that the road network structure can match the travel needs of urban residents better. Aiming at minimizing the total travel time of the whole road network, a mixed-integer bilevel programming model for the reversible lane optimization is constructed as follows:

Upper level:

$$\min Z = \sum_{a \in A} t_a(x_a, l_a) \cdot x_a. \tag{9}$$

$$\text{s.t. } 1 \leq l_a \leq l_{\ddot{a}} - 1 \quad \forall a \in A. \tag{10}$$

$$l_a + l_{\overline{a}} = l_{\ddot{a}}, \quad \forall a \in A, \overline{a} \in A. \tag{11}$$

Lower level:

$$\min \sum_{a \in A} \int_0^{x_a} t_a(\omega, l_a) \mathrm{d}\omega. \tag{12}$$

$$\text{s.t. } \sum_k f_k^{rs} = d_{rs}, \quad \forall (r,s) \in w. \tag{13}$$

$$f_k^{rs} \geq 0, \quad \forall (r,s) \in w. \tag{14}$$

$$x_a = \sum_r \sum_s \sum_k f_k^{rs} \delta_{a,k}^{rs}, \quad \forall a \in A, \tag{15}$$

where ω is the integral variable symbol, f_k^{rs} is the flow on the path k between OD pairs (r,s), d_{rs} is the travel demand between OD pairs (r,s), $\delta_{a,k}^{rs}$ is the correlation coefficient between the path and the section, when the path k passes through the section a, $\delta_{a,k}^{rs} = 1$, otherwise, $\delta_{a,k}^{rs} = 0$; formula (10) shows that the adjustment range of the number of lanes in the section a is $[1, l_{\ddot{a}} - 1]$; formula (11) is the conservation constraint of the number of lanes in the section; formula (13) is the conservation constraint of traffic flow; formula (14) is nonnegative constraint of path flow.

4. Model Solution

Considering the complexity of the solution process for the optimization model of nonlinear mixed-integer bilevel programming problem which includes NP-hard optimization problems (e.g., Karshenas et al. [29], Wang et al. [30], Zhou et al. [31], and Shi et al. [32]), we propose a chaotic particle swarm optimization algorithm, which is a parallel algorithm, starts from the random solution, and finds the optimal solution through iteration. The detailed steps are described as follows:

Step 1. Initialization. Let the number of iterations be η, the maximum allowable number of iterations be $\eta_{\max}$, the particle swarm size be m, the reduction coefficients be z_1 and z_2, respectively, the dynamic delay period be ξ, the maximum speed be $v_{a,\max}$, the inertia weight factor be κ, and the acceleration coefficients be γ_1 and γ_2, respectively. The position $(\cdots, \varphi_{a,\eta}^i, \cdots)$ of the ηth iteration of the $i(i = 1, 2 \cdots m)$th particle corresponds to the state $(\cdots, l_{a,\eta}^i, \cdots)$ of the ηth iteration of the ith reversible lane optimization scheme, the maximum particle position of section a is $\varphi_{a,\max}$, corresponding to the maximum number of lane settings $l_{\ddot{a}} - 1$ of section a, and the travel demand is d_{rs}; each feasible particle initial position $\varphi_{a,0}^i$ and initial speed $v_{a,0}^i$ are randomly generated, the chaotic parameter is μ, and the maximum number of iterations is $\psi_{\max}$.

Step 2. Calculate fitness. For each feasible particle, solve the lower user equilibrium traffic allocation model and then

solve the upper objective function value according to the section flow, that is, the fitness of the particle.

Step 3. Organize the particles in the swarm and update the fitness of the particles in the swarm. Particles are processed subchaotic iteratively $\psi_{\max}$ times using logistic maps. Assuming that the search space element of the same dimension as $(\cdots, \varphi^i_{a,\eta}, \cdots)$ is $Y = (\cdots, y_i, \cdots)$, y_i is the ith component of the vector Y, $y_i \in [0,1]$, and iteration is performed by $y_i^{k+1} = \mu y_i^k (1 - y_i^k)$, when the number of iterations is reached at $\psi_{\max}$, the chaotic sequence $\left\{y_i^j | j = 1, 2, \cdots, k\right\}$ of the ith component $y_i (i = 1, 2, \cdots)$ of the vector Y is obtained. When $\mu = 4$, the chaotic sequence obtained by the logistic maps is in a completely chaotic state, and when $\psi_{\max}$ large enough, the chaotic sequence is able to traverse all the values of the search space.

Step 4. Update the historical optimal location of individuals and groups. For the $i\,(i = 1, 2 \cdots m)$th particle, the individual extremum $pbest^i_{a,\eta}$ is updated with the position corresponding to the current optimal fitness. For particle swarm optimization, the optimal position of all $pbest_{a,\eta}$ is used to update the population extremum $gbest_{a,\eta}$. If $\text{gbest}_{a,\eta}$ does not improve after ξ successive iterations, make $\kappa = z_1 \kappa$, $v_{a,\max} = z_2 v_{a,\max}$.

Step 5. Update the particle velocity according to $v^i_{a,\eta+1} = \kappa v^i_{a,\eta} + \gamma_1 R_1 (pbest^i_{a,\eta} - \varphi^i_{a,\eta}) + \gamma_2 R_2 (gbest_{a,\eta} - \varphi^i_{a,\eta})$, where $v^i_{a,\eta}$ is the velocity of the ηth iteration of the $i\,(i = 1, 2 \cdots m)$th particle, R_1 and R_2 are random numbers between $(0, 1)$, and the velocity of each particle shall be rounded to an integer. If $v^i_{a,\eta+1} > v_{a,\max}$, order $v^i_{a,\eta+1} = v_{a,\max}$.

Step 6. Update the particle position based on $\varphi^i_{a,\eta+1} = \varphi^i_{a,\eta} + v^i_{a,\eta}$. If $\varphi^i_{a,\eta+1}$ does not meet the constraint condition $1 \le \varphi^i_{a,\eta+1} \le \varphi_{a,\max}$, it is discarded and the position of the ith particle is not updated. If the constraint conditions are met, judge the ith particle. If the particle makes no path connection between an OD pair, discard the new position and do not update the position of the ith particle, otherwise update the ith particle to the new position.

Step 7. Terminate the inspection. If the termination condition is satisfied, the iteration is stopped and $gbest_{a,\eta}$ is output as the optimal adjustment scheme. Otherwise, let $\eta = \eta + 1$ and return to Step 1.

5. Calculations and Analysis of Numerical Example

The test road network is shown in Figure 1, which is composed of four nodes and five two-way sections. It is assumed that there are four OD pairs, and the travel demand is $d_{14} = 4560$pcu/h, $d_{41} = 910$pcu/h, $d_{23} = 780$pcu/h, and $d_{32} = 1130$pcu/h. The parameter value of the BPR function is $\alpha = 0.15$ and $\beta = 4$. The characteristic parameters of each section, including free travel time, single-lane capacity, and number of lanes, are shown in Table 2.

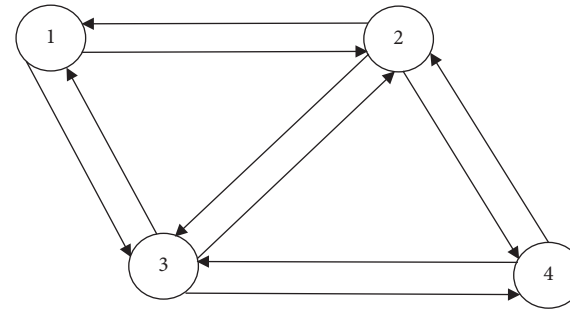

Figure 1: Test road network.

Table 2: Characteristic parameters of each section.

Section	Free travel time (s)	Single-lane capacity (pcu ·h^{-1})	Number of lanes
1–2	95	650	4
2–1	95	650	4
3–1	55	700	3
1–3	55	700	3
2–3	41	700	3
3–2	41	700	3
4–2	55	650	4
2–4	55	650	4
4–3	95	700	3
3–4	95	700	3

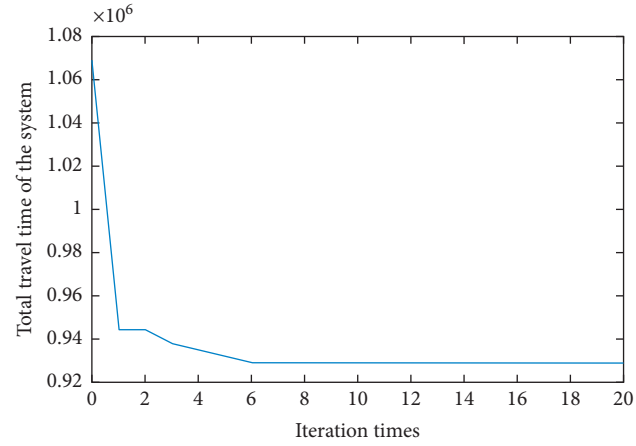

Figure 2: Total travel time of the system changes with iteration times.

For the number of lanes in each section in the example, set $\varphi_{1-2,\max} = 7$, $\varphi_{2-4,\max} = 7$, $\varphi_{1-3,\max} = 5$, $\varphi_{2-3,\max} = 5$, $\varphi_{3-4,\max} = 5$, $v_{1-2,\max} = 7$, $v_{2-4,\max} = 7$, $v_{1-3,\max} = 5$, $v_{2-3,\max} = 5$, and $v_{3-4,\max} = 5$. At the same time, in order to improve the convergence speed of particle swarm optimization algorithm and ensure its effective convergence, set $m = 20$, $z_1 = 0.9$, $z_2 = 0.9$, $\gamma_1 = 1.8$, $\gamma_2 = 1.8$, $\xi = 6$, $\kappa = 1.3$, $\eta_{\max} = 20$, $\mu = 4$, and $\psi_{\max} = 20$. The total travel time of the system under the reversible lane optimization scheme changes with iteration times as shown in Figure 2.

The comparison of characteristic values such as lane number, capacity, flow, and travel time of each section before and after reversible lane optimization is shown in

Table 3: Characteristic values of sections before and after optimization.

Section	Number of lanes		Capacity (pcu ·h^{-1})		Flow (pcu ·h^{-1})		Travel time (s)	
	Before	After	Before	After	Before	After	Before	After
1–2	4	7	2173	3625	2368	2537	115.10	98.42
2–1	4	1	2173	650	495	438	95.04	97.94
3–1	3	1	1822	700	415	472	55.02	56.70
1–3	3	5	1822	2861	2192	2023	72.28	57.06
2–3	3	2	1822	1309	780	780	41.21	41.78
3–2	3	4	1822	2341	1351	1151	42.86	41.36
4–2	4	1	2173	650	495	438	55.02	56.70
2–4	4	7	2173	3625	2590	2559	71.65	57.05
4–3	3	1	1822	700	415	472	95.04	97.94
3–4	3	5	1822	2861	1970	2001	114.48	98.41

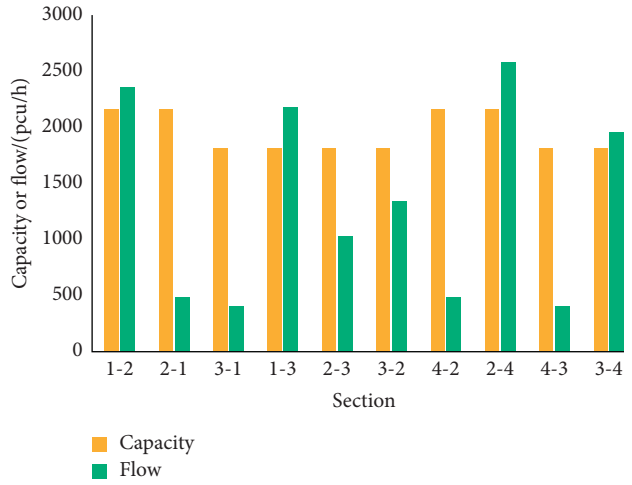

Figure 3: The capacity and flow of each section before reversible lane optimization.

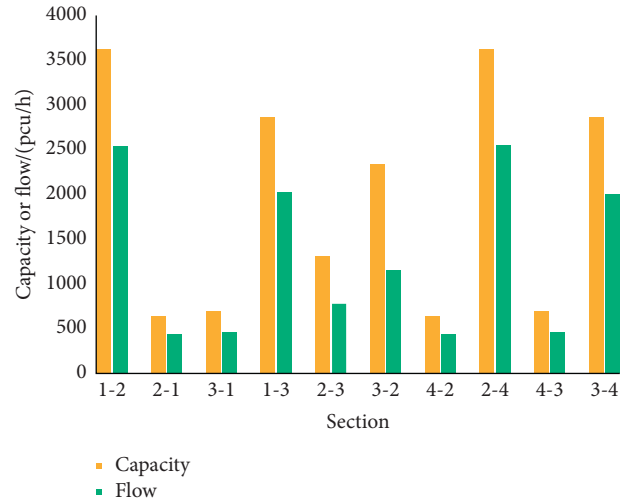

Figure 4: The capacity and flow of each section after reversible lane optimization.

Table 3. For comparison, the capacity and flow of each section before reversible lane optimization are shown in Figure 3. The capacity and flow of each section after reversible lane optimization are shown in Figure 4. The

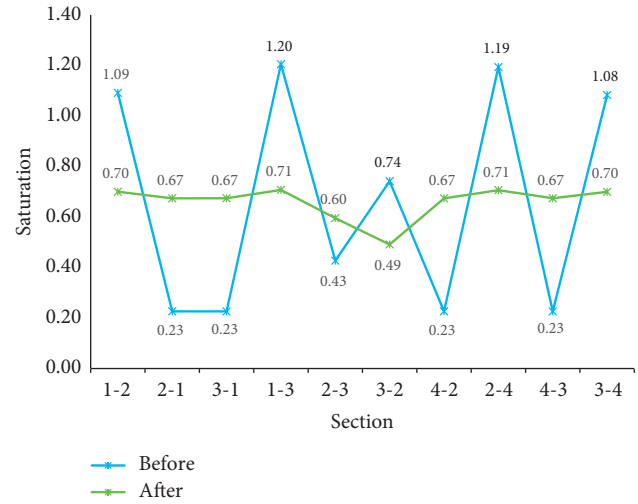

Figure 5: Saturation of sections before and after optimization.

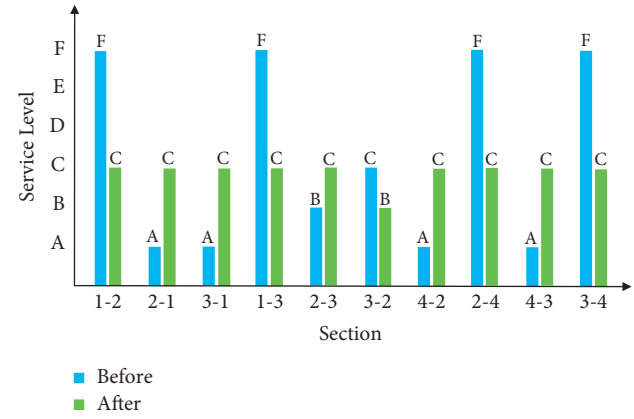

Figure 6: Service level of sections before and after optimization.

saturation comparison of each section before and after the optimal setting of reversible lane is shown in Figure 5. The service level of each section before and after the optimal setting of reversible lane is shown in Figure 6.

Before the optimal setting of reversible lanes, the traffic flow of sections 1–2, 2–4, 1–3, and 3–4 in heavy traffic flow direction is larger than the capacity, and the saturation exceeds 1, which is F service level, and the sections are very

Table 4: Route travel time before and after optimization.

OD pair	Route/in node order	Route travel time/s			Total time/s		
		Before	After	Difference	Before	After	Difference
(1,4)	1–2–4	186.8	155.5	−31.3	851808	709080	−142728
	1–2–3–4	270.8	238.6	−32.2			
	1–3–4	186.8	155.5	−31.3			
	1–3–2–4	186.8	155.5	−31.3			
(4,1)	4–2–1	150.1	154.6	4.5	136591	140686	4095
	4–2–3–1	151.3	155.2	3.9			
	4–3–1	150.1	154.6	4.5			
	4–3–2–1	232.9	237.2	4.3			
(2,3)	2–3	41.2	41.8	0.6	32136	32604	468
	2–4–3	166.7	155.0	−11.7			
	2–1–3	167.3	155.0	−12.3			
(3,2)	3–2	42.9	41.4	−1.5	48477	46782	−1695
	3–1–2	150.1	154.6	4.5			
	3–4–2	169.5	155.1	−14.4			

congested. The flow of sections 2–1, 4–2, 3–1, and 4–3 in the light traffic flow direction is much more smaller than the capacity, and the saturation is less than 0.25, which is A service level, and the road resources are not fully utilized. The traffic tide phenomenon in 2-way sections is obvious, and the problems of traffic congestion and idle road resources are prominent.

After the optimal setting of reversible lanes, the number of lanes of the section in the heavy traffic flow direction increases, the section's capacity increases accordingly, and the travel time decreases significantly, while the number of lanes of the section in the light traffic flow direction decreases, the section's capacity decreases accordingly, and the travel time increases slightly. The saturation of each section is between 0.45 and 0.75, with the variance decreased from 0.175 to 0.004, the saturation is more balanced, the sections are all at the service level of B or C, and there is neither excessive congestion nor idle road resources.

It shows that the reversible lane optimization scheme can make full use of the idle road resources in the light traffic flow direction to improve the capacity of the section in the heavy traffic flow direction, adjust the distribution of flow on the road network, reduce the travel time of sections in the heavy traffic flow direction significantly, balance the saturation and service level of sections, and alleviate the coexistence of traffic congestion and idle road resources caused by traffic tide phenomenon effectively.

The route travel time between OD pairs before and after reversible lane optimization is shown in Table 4. The total travel time of the system and between OD pairs before and after reversible lane optimization is shown in Figure 7.

From the perspective of equilibrium travel time between OD pairs, although the travel time between OD pairs (4,1) with smaller demand increased from 150.1s to 154.6s, and the travel time between OD pairs (2,3) also increased from 41.2s to 41.8s, the travel time between OD pairs (1,4) with larger demand decreased from 186.8s to 155.5s, and the travel time between OD pairs (3,2) also decreased from 42.9s to 41.4s. It shows that reversible lane optimization can adjust more road resources to travelers between OD pairs with larger demand and make the road network structure better match the travel demand.

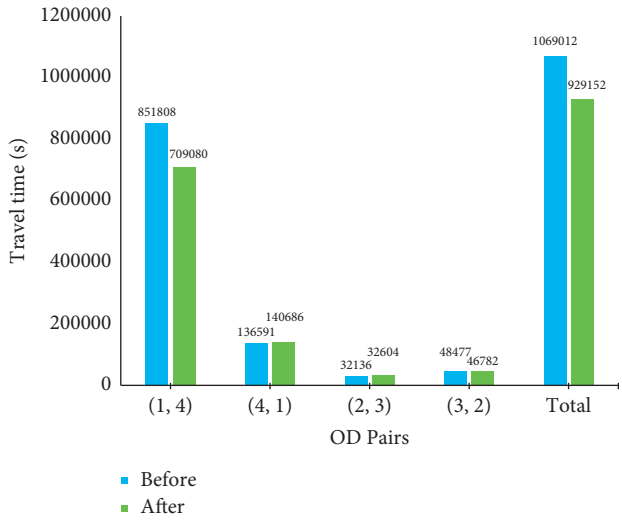

Figure 7: Total travel time of the system and between OD pairs before and after optimization.

From the perspective of the total travel time between OD pairs, although the total travel time between OD pairs (4,1) with smaller demand increased from 136591s to 140686s, and the total travel time between OD pairs (2,3) also increased from 32136s to 32604s, the travel time between OD pairs (1,4) with larger demand decreased from 851808s to 709080s, and the travel time between OD pairs (3,2) also decreased from 48477s to 46782s. The increase of total travel time between OD pairs with smaller demand is smaller, and the decrease of total travel time between OD pairs with larger demand is larger. Finally, the total travel time of the system decreases from 1069012s to 929152s, with a decrease of 13.08%, indicating that the effect of reversible lane optimization on reducing the total travel time of the system is obvious.

6. Conclusions

This manuscript established a mixed-integer bilevel programming model for reversible lane optimization, considering the influence of vehicle lane-changing on traffic

capacity which enhances the accuracy of the model, and proposed a chaotic particle swarm optimization algorithm for this model. Numerical examples verified the effectiveness of the proposed optimization scheme and its solution algorithm and showed the influences of reversible lane optimization on capacity, flow, travel time, saturation and service level of sections, route travel time between OD pairs, and total time of the system. The results showed that the reversible lane optimization can make the road network structure better match the travel demand, adjust the distribution of flow on the road network, reduce the travel time of sections in the heavy traffic flow direction, balance the saturation and service level of sections, and reduce the total travel time of the system obviously.

Beyond the above preliminary research, there are many interesting avenues for further study such as a couple of ablation studies may be added to evaluate the effects of the key parameters of the proposed method on the performance, the setting of the signal light may significantly affect the effect of the reversible lane optimization scheme, and an ongoing extension of this study is to integrate the signal control into our proposed model.

Data Availability

The data used to support the findings of this study are available from the corresponding author upon request.

Conflicts of Interest

The authors declare that there are no conflicts of interest regarding the publication of this paper.

Acknowledgments

This research work was supported by the Hunan Provincial Natural Science Foundation of China (Grant nos. 2021JJ40025 and 2019JJ50210) and Scientific Research Foundation of Hunan Provincial Education Department (Grant nos. 20A093 and 18C0859).

References

[1] X. Li and J.-Q. Sun, "Signal multiobjective optimization for urban traffic network," *IEEE Transactions on Intelligent Transportation Systems*, vol. 19, no. 11, pp. 3529–3537, 2018.

[2] C. K. Wong and S. C. Wong, "Lane-based optimization of signal timings for isolated junctions," *Transportation Research Part B: Methodological*, vol. 37, no. 1, pp. 63–84, 2003.

[3] Y. H. Jiang and L. X. Bao, "Study on setting of reversible lanes near intersection between one-way and two-way traffic," *Journal of Shanghai Jiaotong University*, vol. 45, no. 10, pp. 1562–1566, 2011.

[4] Q. Yu and R. Tian, "Research on reversal lane application method of urban road network based on the bi-level programming," *Advances in Intelligent Systems and Computing*, vol. 279, pp. 983–992, 2014.

[5] B. Wolshon and L. Lambert, *Convertible roadways and lanes: a synthesis of highway practice*, Vol. 340, Transportation Research Board National Research Council, , Washington, DC, USA, 2004.

[6] A. Golub, "Perceived costs and benefifits of reversible lanes in Phoenix, Arizona," *ITE Journal*, vol. 82, no. 2, pp. 38–42, 2012.

[7] P. Zhang, W. Li, and Y. Chang, "Reserve capacity model for urban road network with reversible lanes," *Journal of Southwest Jiaotong University*, vol. 45, no. 2, pp. 255–260, 2010.

[8] X. Li, J. Chen, and H. Wang, "Study on flow direction changing method of reversible lanes on urban arterial roadways in China," *Procedia - Social and Behavioral Sciences*, vol. 96, pp. 807–816, 2013.

[9] M. Hausknecht, T. C. Au, P. Stone, D. Fajardo, and T. Waller, "Dynamic lane reversal in traffic management," in *Proceedings of the 2011 14th International IEEE Conference on Intelligent Transportation Systems (ITSC)*, pp. 1929–1934, IEEE, Washington, DC, USA, October 2011.

[10] B. Wolshon and L. Lambert, "Reversible lane systems: synthesis of practice," *Journal Of Transportation Engineering*, vol. 132, no. 12, pp. 933–944, 2006.

[11] H. Waleczek, J. Geistefeldt, D. Cindric-Middendorf, and G. Riegelhuth, "Traffic flow at a freeway work zone with reversible median lane," *Transportation Research Procedia*, vol. 15, pp. 257–266, 2016.

[12] L. Yue, T. D. Xu, H. P. Xia, and Y. C. Du, "Reversible lane design for Shanghai world expo 2010," *Urban Transport of China*, vol. 8, no. 2, pp. 25–30, 2010.

[13] W. Y. Wang, Y. Jiang, Y. Peng, Y. Zhou, and Q. Tian, "Simheuristic method for the reversible lanes allocation and scheduling problem at smart container terminal gate," *Journal of Advanced Transportation*, vol. 2018, Article ID 1768536, 14 pages, 2018.

[14] J.-B. Sheu and S. G. Ritchie, "Stochastic modeling and real-time prediction of vehicular lane-changing behavior," *Transportation Research Part B: Methodological*, vol. 35, no. 7, pp. 695–716, 2001.

[15] G. Xiao, H. Zhang, N. Sun, Y. Chen, J. Shi, and Y. Zhang, "Cooperative Bargain for the Autonomous Separation of Trafic Flows in Smart Reversible Lanes," *Complexity*, vol. 2019, Article ID 2893732, 12 pages, 2019.

[16] L. Mao, W. Li, and P. Hu, "Design of real-time dynamic reversible lane in intelligent cooperative vehicle infrastructure system," *Journal of Advanced Transportation*, vol. 2020, Article ID 8838896, 8 pages, 2020.

[17] T. L. Magnanti and R. T. Wong, "Network design and transportation planning: models and algorithms," *Transportation Science*, vol. 18, no. 1, pp. 1–55, 1984.

[18] F. Shi, H. Y. Su, and X. Wang, "Design of reversible lanes with tidal flow on road network," *Journal of Transportation Systems Engineering and Information Technology*, vol. 15, no. 4, pp. 57–62, 2015.

[19] Z. Y. Gao, H. Z. Zhang, and H. J. Sun, "Bi-level programming models, approaches and applications in urban transportation network design problems," *Journal of Transportation Systems Engineering and Information Technology*, vol. 4, no. 1, pp. 35–44, 2004.

[20] H. Z. Zhang and Z. Y. Gao, "Optimization approach for traffic road network design problem," *Chinese Journal of Management Science*, vol. 15, no. 2, pp. 86–91, 2004.

[21] T. Lu, Z. Yang, D. Ma, and S. Jin, "Bi-level programming model for dynamic reversible lane assignment," *IEEE Access*, vol. 6, pp. 71592–71601, 2018.

[22] Z. Di and L. X. Yang, "Reversible lane network design for maximizing the coupling measure between demand structure and network structure," *Transportation Research Part E: Logistics and Transportation Review*, vol. 141, p. 102021, 2020.

[23] L. Conceio, G. Correia, and J. P. Tavares, "The reversible lane network design problem (RL-NDP) for smart cities with automated traffic," *Sustainability*, vol. 12, no. 3, p. 1226, 2020.
[24] J. R. Cai, Z. X. Huang, and L. X. Wu, "Optimization of reversible lane based on autonomous vehicles," *Journal of Highway and Transportation Research and Development*, vol. 35, no. 7, pp. 136–150, 2018.
[25] X. B. Yang, N. Zhang, and Y. Guan, "Behavior based analysis of the relationship between expressway capacity and number of lanes," *China Civil Engineering Journal*, vol. 43, no. 10, pp. 104–110, 2009.
[26] X. Li and J.-Q. Sun, "Studies of vehicle lane-changing dynamics and its effect on traffic efficiency, safety and environmental impact," *Physica A: Statistical Mechanics and Its Applications*, vol. 467, no. 1, pp. 41–58, 2017.
[27] X. B. Yang and N. Zhang, "Mathematical analysis of effects of lanes' number on expressway capacity," *Journal of Wuhan University of Technology*, vol. 32, no. 4, pp. 603–606, 2008.
[28] W. Wang and X. C. Guo, *Traffic engineering*, Vol. 156, Southeast University Press, Nanjing, China, 2009.
[29] H. Karshenas, R. Santana, C. Bielza, and P. Larranaga, "Multiobjective estimation of distribution algorithm based on joint modeling of objectives and variables," *IEEE Transactions on Evolutionary Computation*, vol. 18, no. 4, pp. 519–542, 2014.
[30] S.-Y. Wang and L. Wang, "An estimation of distribution algorithm-based memetic algorithm for the distributed assembly permutation flow-shop scheduling problem," *IEEE Transactions on Systems, Man, and Cybernetics: Systems*, vol. 46, no. 1, pp. 139–149, 2016.
[31] F. Zhou, J. H. Wu, Y. Xu, and C. Yi, "Optimization scheme of tradable credits and bus departure quantity for travelers' travel mode choice guidance," *Journal of Advanced Transportation*, vol. 2020, Article ID 6665161, 8 pages, 2020.
[32] W. Shi, W.-N. Chen, Y. Lin, T. Gu, S. Kwong, and J. Zhang, "An adaptive estimation of distribution algorithm for multipolicy insurance investment planning," *IEEE Transactions on Evolutionary Computation*, vol. 23, no. 1, pp. 1–14, 2019.